Optics Communications 526 (2023) 128890

Contents lists available at ScienceDirect

Optics Communications

journal homepage: www.elsevier.com/locate/optcom

Simple and stable gas–liquid two-phase optical fiber sensor for acetone based on cholesteric liquid crystal

Xiujuan Liu [a], Chaofeng Qu [a], Sijie Zhou [a], Wenzhu Cao [a], Minxing Xu [a], Yongjun Liu [a,b,*]

[a] Key Lab of In-fiber Integrated Optics, Ministry Education of China, Harbin Engineering University, Harbin 150001, China
[b] State Key Laboratory of Applied Optics, Changchun Institute of Optics, Fine Mechanics and Physics, Chinese Academy of Sciences, Changchun 130033, China

ARTICLE INFO

Keywords:
Optical fiber sensing
Liquid crystal
Temperature compensation

ABSTRACT

We propose an optical fiber sensor based on cholesteric liquid crystals (CLCs) for monitoring the concentration of acetone in a gas–liquid two-phase environment. The sensor consists of two optical fiber probes, which can compensate the temperature when detecting the acetone concentration. The results showed that the temperature sensitivity of the two cholesteric liquid crystals are 2.44 nm/°C and 5.08 nm/°C, respectively. In gas-phase and liquid-phase environments, the sensitivities of cholesteric liquid crystals to acetone are 46.95 nm/mmol L^{-1} and 8.43 nm/%, respectively. In addition, when the temperature fluctuates greatly, the sensor can perform temperature compensation. The proposed sensor has the advantages of small size, simple manufacture and convenient measurement method, providing convenience for the monitoring of acetone leakage in industrial production.

1. Introduction

Acetone, one of the common volatile organic compounds VOCs in industry, is mainly used as a solvent for explosives, rubber, tanning, paint and other chemicals. It also serves as an important raw material for the synthesis of ketone, iodoform, epoxy resin and others [1]. As the simplest and smallest ketone [2–4], acetone is flammable. At temperatures above the flash point (20 °C), air mixtures containing 2.5%–12.8% acetone may explode or cause flash fires [5]. In addition, acetone is a toxic and harmful substance, resulting in anesthetic effect to central nervous system which makes people feel fatigue, nausea and dizziness, and in severe cases, it leads to vomiting, convulsion and coma. Owing to its irritation to skin and mucosa, long-term exposure to acetone vapor can cause pharyngitis, bronchitis and dermatitis [5–8]. Acetone is easily soluble in water [9], and acetone content in urine of healthy women will increase during ovulation [10,11], of which the study has clinical significance for ovulation research. Acetone found in groundwater causes the environmental pollution as well [12]. Therefore, monitoring of acetone in solution is as important as that in air. So far, many methods have been proposed to detect the acetone concentration. Metal oxide semiconductors (MOS) like WO_3 [13] and SnO_2 [14] are widely applied to gas sensing. However, MOS-based sensors usually exhibit long response time and recovery time to acetone, are greatly affected by humidity, high operating temperature (125–500 °C) and can only be used to gas measurement. Other methods such as Gas chromatography mass spectrometry (GC–MS) [15], resistance-based gas sensors [16] and fluorescence quenching method (FQ) [17] require huge instruments and the fluorescence lifetime is short. There are also some known materials sensitive to acetone, including polydimethylsiloxane/divinylbenzene (PDMS/DVB), liquid crystal (LC) polymer network, etc. Some studies of the LC sensors have reported that the molecular structure of LC has special functional groups whose direction changes with the formation of specific chemical bonds. Therefore, VOCs can be detected using liquid crystals. Chang et al. presented a novel hydrogen-bridged cholesteric liquid crystal (CLC) polymer networks with a porosity [18]. This material is used to distinguish VOCs. Xu et al. showed that the optical texture of a layer of liquid crystal 4-cyano-4'-pentylbiphenyl (5CB) supported on a thiol-sensitive layer can be applied to detect VOCs [19]. Chang et al. used colorimetry of cholesterol liquid crystals to distinguish acetone from toluene [20]. Researchers usually make an LC cell to detect. According to the color change of the liquid crystal, the presence of acetone is qualitatively detected. Our research group can quantitatively detect acetone in gases and liquids by coating LCs on fiber optic sensing probes [21,22]. For the first time, we have implemented a gas-liquid fiber optic sensing probe for detecting VOCs.

We intend to design a sensor that is smaller, easy to manufacture and can work in both gas and liquid phase. The characteristics of optical fiber sensors meet above requirements. The introduction of CLCs into VOCs sensing devices as the sensitive material usually takes advantage of the fact that the presence of VOCs will cause the helical twisting power of the chiral dopant to change due to the reaction with analyte, or physical expansion of the system changes as the order of the liquid

* Corresponding author at: .
E-mail address: liuyj@hrbeu.edu.cn (Y. Liu).

https://doi.org/10.1016/j.optcom.2022.128890
Received 29 April 2022; Received in revised form 11 July 2022; Accepted 11 August 2022
Available online 19 August 2022
0030-4018/

phase changes, and eventually the helical pitch changes due to the absorption of analyte [23]. CLCs are characterized by their helical structure. The molecules in each layer have an average orientation axis, rotating a small angle from one layer to another. The selective reflection wavelength and reflection bandwidth of CLCs are expressed as [18]:

$$\Delta\lambda = \Delta n \times p \tag{1}$$

where Δn is birefringence, p is the helical pitch which can be changed by external stimuli such as temperature, electricity and chemical bonds. The helical pitch usually gets influenced (expansion or contraction) when the molecular structure of CLCs is modified to absorb special analytes. These influences consequently lead to the real-time changes in reflection wavelength according to Eq. (1). We developed a gas–liquid two-phase sensor by integrating CLCs into optical fiber. The wavelength shifts depending on the degree of helical pitch changes were accurately monitored by a spectrometer while acetone was absorbed by CLCs, then the acetone concentration got measured.

2. Materials and methods

2.1. Materials

Materials used in this experiment: Poly dimethyl siloxane (PDMS), UV glue, glycerin, cholesterol-based derivatives. All materials were purchased from Beijing in no Chem Science &Technology Co, Ltd. Preparation of PDMS: The PDMS and curing agent are mixed in a weight ratio of 8:1. Preparation of cholesterol-based derivatives: The first type of liquid crystal (CLC1) was prepared by mixing 14 wt% cholesterol chlorine, 67.2 wt% cholesteryl oleic acid carbonate, and 18.8 wt% cholesterol chloroformate. The second liquid crystal (CLC2) consisted of 15.2 wt% cholesterol chlorine, 54.4 wt% cholesteryl oleic acid carbonate, and 30.4 wt% cholesterol chloroformate. CLC1 is used for temperature compensation and CLC2 for acetone sensing. The three different mixtures were then heated to 100 °C, treated by ultrasonic at 80 °C for 5 min, and cooled naturally to room temperature at 25 °C.

2.2. Methods

The experimental setup shown in Fig. 1(a) is made up of a 2 × 2 multimode fiber (MMF) coupler, an ocean spectrometer (OSA), a halogen lamp and computer. The two output fibers of coupler (an inner diameter of 62.5 μm and outer diameter of 125 μm) are firstly cut with an optical fiber cutter to access flat end faces, and hollow quartz capillaries (HQC) of an appropriate length (an inner diameter of 75 μm and outer diameter of 150 μm) are separately welded. A suitable length of HQC is otherwise used for injection device whose one end is connected to a syringe and fixed with UV glue, the other end is fused with flame and pulled until the outer diameter decreases to 10 μm. With the syringe, CLC1, glycerin and UV glue are successively injected into welded HQC through the tapered capillary in order to make a temperature probe as shown in Fig. 1(b), UV glue is then cured by UV lamp (20000μW/cm^2). We have confirmed that glycerin and UV glue can seal off CLC1 from external acetone. The HQC of the other fiber is filled with CLC2 and PDMS to make a gas probe shown in Fig. 1(c). PDMS is very temperature-insensitive and chemically inert, allowing the passage of acetone molecules but not water molecules and ions. CLC2 can thereby absorb acetone in the air and water. The white light from the halogen lamp is output to temperature probe and gas probe through the MMF coupler, and the ends of two probes are put in a closed air chamber. OSA (a spectral range of 185–1100 nm and resolution of 0.14 nm) and a computer are responsible for receiving the reflected light from CLCs and record spectra, then analyze the wavelength shifts caused by acetone and temperature changes.

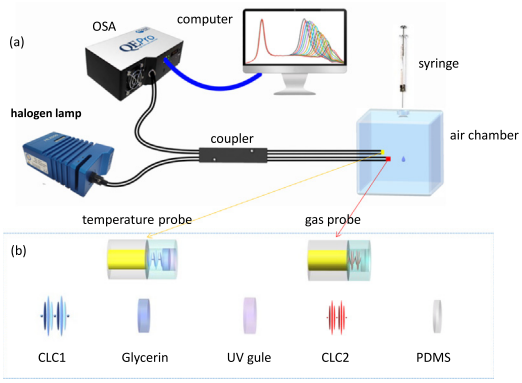

Fig. 1. Schematic diagram of (a) the experimental device; (b) the temperature probe (CLC1) and (c) gas probe (CLC2).

3. Experimental results and discussion

3.1. Experimental

It is reported that volatile organic gases can swell PDMS [24]. Therefore, we studied the effect of cured PDMS on CLC in the measurement. We prepared two probes, one containing CLC1 was named No. 1, and the other containing CLC1 with the same thickness and PDMS was named No. 2. They were joined to the 2 × 2 MMF coupler of experimental device. The results are shown in Fig. 2 (a), in which the black line is the reflection peak of No. 1, the red line is from No. 2, and the blue line named No. 3 represents the superposition of reflection peaks from No. 1 and No. 2. It is observed that the reflection intensity of No. 2 is higher than No. 1. This is due to the anchoring effect of PDMS on CLC1 molecular arrangement [25]. Next acetone was added for testing. Acetone liquid was added drop by drop to the closed air chamber using a micro syringe. Acetone liquid volatilizes naturally in a closed air chamber. After a drop of acetone (2 mg) is completely volatilized, the concentration of gas-phase acetone in the air chamber changes from 0 ppm to 2030 ppm. Acetone is a liquid with a purity of 99 and a closed chamber size of 400 ml. The weight of each drop of liquid acetone is 2 mg, and the time for complete evaporation is 1 min. The result is shown in Fig. 2 (b). As the acetone concentration increases, the No. 3 reflection spectrum shifts to longer wavelength. After reaching the maximum, the acetone concentration is then restored to 0, and No. 3 reflection peak returns to its initial position. It can be concluded from the process that the center wavelengths of the reflection peaks of No. 1 and No. 2 have the same and synchronized changes in response to acetone because No. 3 spectrum describes the combined reflection from two probes. Consequently, cured PDMS has no effect on the measurement of acetone.

To explore whether the thickness of CLC affects the sensitivity of probe, three probes with different thickness of CLC (20 μm, 40 μm and 60 μm) were prepared for experiment. Fig. 3(a) shows their respective reflection spectra, images under the optical microscope and polarizing microscope (POM). It can be seen that the intensity of reflection peak increases with thickening CLC. Fig. 3(b) shows the relationships between acetone concentration and center wavelength shift of reflection peaks. The sensitivities of three probes we get by fitting curves are 44.80 nm/mmol L^{-1}, 46.66 nm/mmol L^{-1} and 47.75 nm/mmol L^{-1} corresponding to the CLC thicknesses of 20 μm, 40 μm and 60 μm, and the linear fitting correlations are 0.998, 0.999 and 0.999. Through our many experiments, we also found the spectrum of probe with thicker CLC often spends more time reaching a steady state. The reason for this may be that it takes time for the acetone molecule to diffuse into CLC. Therefore, the probe with a LC thickness of 40 μm was selected for subsequent experiments. The experiments were carried out at room temperature (25 °C).

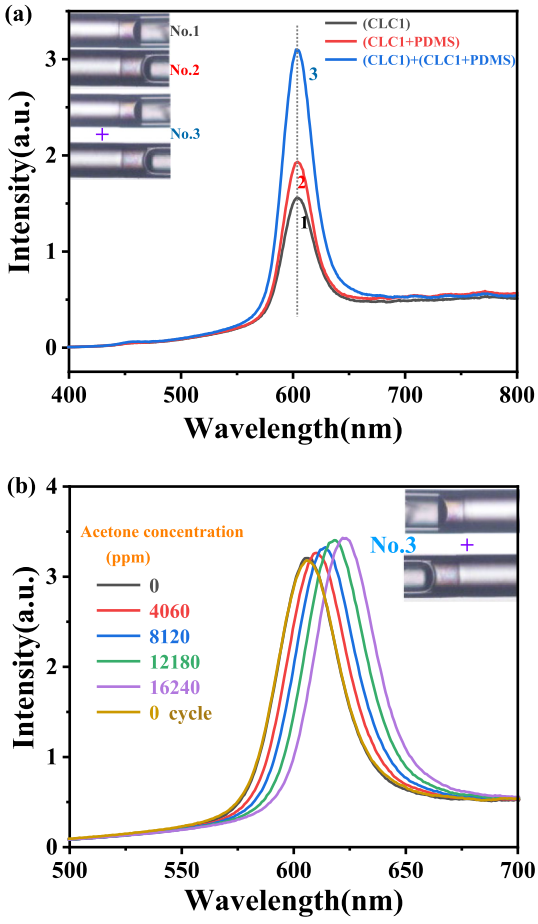

Fig. 2. (a) Reflection spectra of the probes with and without PDMS and their images under an optical microscope; (b) The wavelength shifts of reflection peak generated by two probes with the changing acetone concentration.

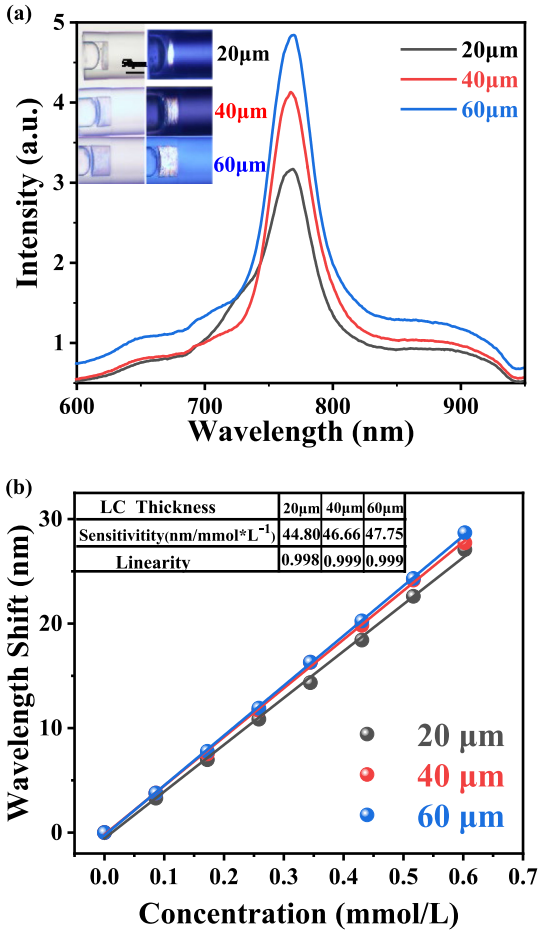

Fig. 3. (a) The reflection peaks of gas probes with CLC thicknesses of 20 μm, 40 μm, 60 μm and their optical micrographs; (b) Sensitivities of three probes in acetone measurement and linear fitting results.

3.2. The sensing characteristics of sensor in the air

In the following experiments, a gas sensor with the CLC thickness of 40 μm was used to determine the maximum detection range and detection limit for acetone gas. All other things being equal, the acetone concentration was changed. The detection scope was obtained by adding 2 mg of acetone into air chamber (2030 ppm) at a time until the reflection peak was destroyed. Analyzing the results shown in Fig. 4(a), we observe that the reflection peak of gas probe (CLC2) is red-shifted and at last becomes immobile and unidentifiable. Over the response range the maximum acetone concentration recorded is 2.1525 mmol/L that the concentration is increased as little as 44 ppm each time. When the acetone concentration rises from 0 to 308 ppm, a small shift of CLC2 reflection peak just takes place. According to results shown in Fig. 4(b), the gas probe has a detection limit of 308 ppm, generating a center wavelength shift of 1.5 nm. The inset is a partial enlarged view of CLC2 reflection spectra with the variation of concentration. In theory, the calculation formula of the limit of detection (LOD) is as follows [26]:

$$LOD = 3S_a/b \tag{2}$$

where S_a is the standard deviation, b is the slope of the calibration curve. After calculation, the theoretical value of the sensor's LOD is 293 ppm.

Actually, the liquid crystal is affected by temperature [27], so we use the CLC1 probe to monitor the change of ambient temperature in real time. Besides, the temperature detection is devoted to compensating gas probe for its deviation caused by temperature. Fig. 5(a) shows the reflection spectra of CLC1 and CLC2 at different temperatures. When the temperature rises from 24 °C to 40 °C, the two reflection peaks both shift towards longer wavelength. We subsequently plot Fig. 5(b), the temperature sensitivities of CLC1 and CLC2 calculated by linear fitting is 2.44 nm/°C and 5.08 nm/°C, and the correlation coefficient R2 is 0.999 and 0.998, respectively.

The black data points in Fig. 6 represent the wavelength drift of CLC1 reflection peak with temperature fluctuation. In order to eliminate the influence of ambient temperature on the detection of acetone gas, the solution is as follows [28]:

$$\Delta\lambda_{\mathrm{CLC2}_{\mathrm{acetone}}} = \Delta\lambda_{\mathrm{CLC2}} - \frac{\Delta\lambda_{\mathrm{CLC1}} \cdot S_{\mathrm{CLC2}}}{S_{\mathrm{CLC1}}} \tag{3}$$

In this formula, S_{CLC_1} and S_{CLC_2} refer to the sensitivities of CLC1 and CLC2 to temperature respectively, $\Delta\lambda_{\mathrm{CLC}_1}$ and $\Delta\lambda_{\mathrm{CLC}_2}$ are the wavelength shifts of CLC1 and CLC2 actually obtained in acetone measurement. $\Delta\lambda_{\mathrm{CLC}_2}$ acetone refers to the independent wavelength shifts of CLC2 only caused by acetone. Through this calculation method the performance of gas probe is avoided from being affected by temperature to a certain extent. In Fig. 6, the blue points reveal the irregular reflection wavelengths of CLC2 as a joint result of temperature and acetone, and the red points represent the wavelength drift of CLC2 after temperature compensation. Fig. 6 distinctly shows the measurement results of acetone with the maximum temperature fluctuations of around

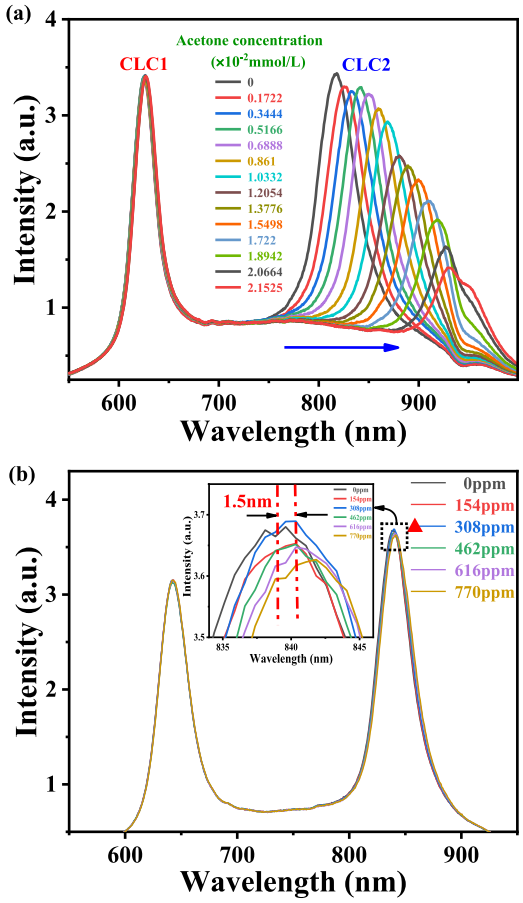

Fig. 4. Reflection spectra of CLCs under different acetone concentrations : (a) detection range; (b) detection limits.

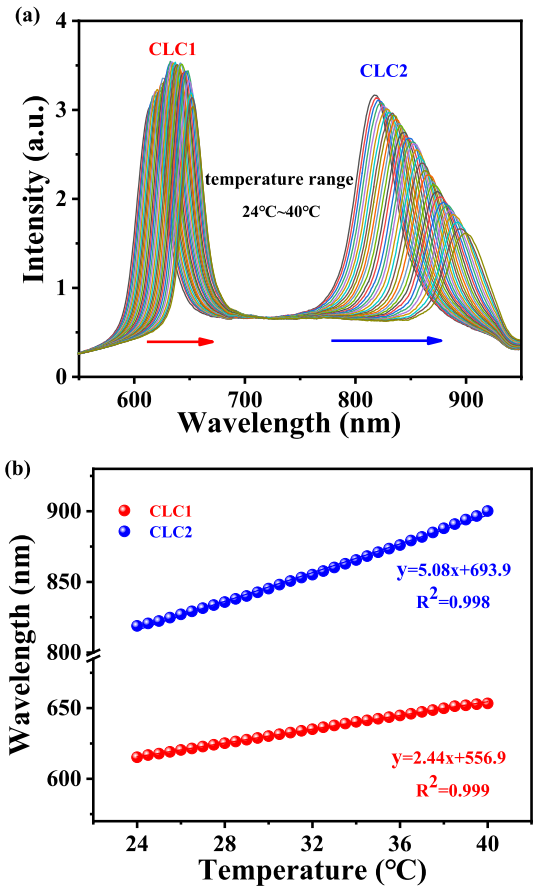

Fig. 5. Responses of the sensor at different temperatures: (a) reflection spectra of CLCs; (b) temperature dependences of reflective center wavelength.

1 °C (a), 3 °C (b), 4 °C (c) and 5 °C (d), respectively. These results suggest that after temperature compensation, the reflective wavelength shift of CLC2 has a relatively good linear relationship with acetone concentration, which is reflected in the correlation coefficients of 0.997, 0.994, 0.993 and 0.950. As can be seen from the decreasing linearity, a large temperature fluctuation diminishes the effect of temperature compensation, reducing the accuracy of gas probe. The proposed sensor with two probes has been shown to monitor temperature and acetone vapor in real time, and still maintains a high degree of linearity and stability when ambient temperature changes.

The influence of humidity on the sensor has also been explored. In this process we put probes in an air chamber, changed the inside humidity and kept the temperature constant. The results are shown in Fig. 7 as the relative humidity increased from 29% to 75%. By analyzing the reflection spectra of CLCs in Fig. 7(a) as well as the relationships between humidity and reflective center wavelength in Fig. 7(b), we observed a wavelength shift of 0.33 nm from gas probe. This obviously indicates that the relative humidity has a very tiny effect on the sensor which can be ignored.

3.3. The sensing characteristics of sensor in liquid

The probes are equipped to work under liquid condition, they were immersed in the pre-prepared aqueous solutions of acetone. The maximum acetone concentration that the sensor can detect is 13% according to measurement result shown in Fig. 8(a). After putting the probes back in water and waiting a while, we found the reflection peak of CLC2 shifts back to original position as well, and its intensity decreases slightly than before. Because acetone has an effect on the order of CLC molecules. The inset in Fig. 8(a) is an enlarged view of the reflection spectra with the probes placed in solutions of 0%, 13%, and 0% acetone in order. When studying the detection limit of the sensor for acetone in solution, we prepared the detected solutions of lower concentrations and recorded a minimum concentration that can move the reflection peak. As shown in Fig. 8(b) and its partial enlarged view, the wavelength shift of 2.3 nm corresponds to the detection limit of 6.096×10^{-6}%. Therefore, the sensor is available for monitoring acetone in solution with the maximum detectable concentration of 13% and the detection limit of 6.096×10^{-6}%.

3.4. Response time and stability of sensor

Fig. 9(a) exhibits the response time of the sensor to different concentrations of acetone in aqueous solution. As the acetone concentration increases by 1%, in multiple measurements the difference in response time is small, that is, its influence on acetone detection is negligible. Fig. 9(b) shows the repeatability of the sensor working in solution. We repeatedly measured the solution of 0% and 1% acetone, the reflection peak of CLC2 meanwhile shifted back and forth. From the variation curve of wavelength shift, we observe the maximum wavelength deviations of 0.032 nm and 0.226 nm when the acetone concentration C is 0% and 1%. The results show that this sensor has good reversibility and repeatability for measuring acetone in solution.

The repeatability of the sensor in air is also studied and shown in Fig. 9(c). Based on the same principle, measurements were conducted

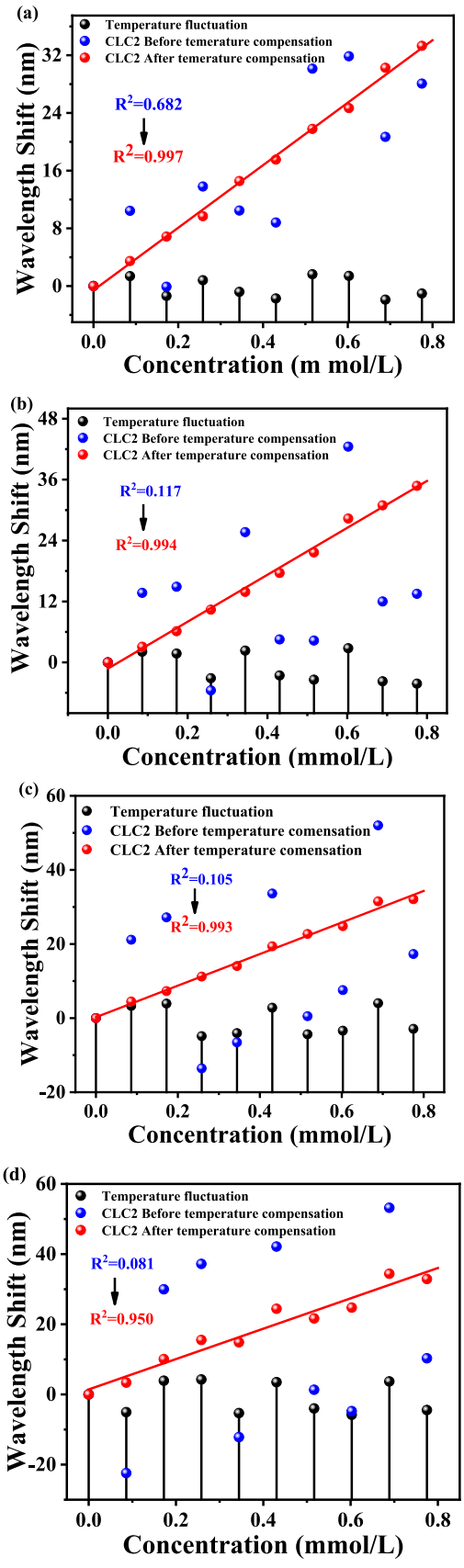

Fig. 6. Relationships between wavelength variation of CLC2 reflection and acetone concentration before and after temperature compensation when the ambient temperature fluctuates about 1 °C (a); 3 °C (b); 4 °C (c); 5 °C (d)

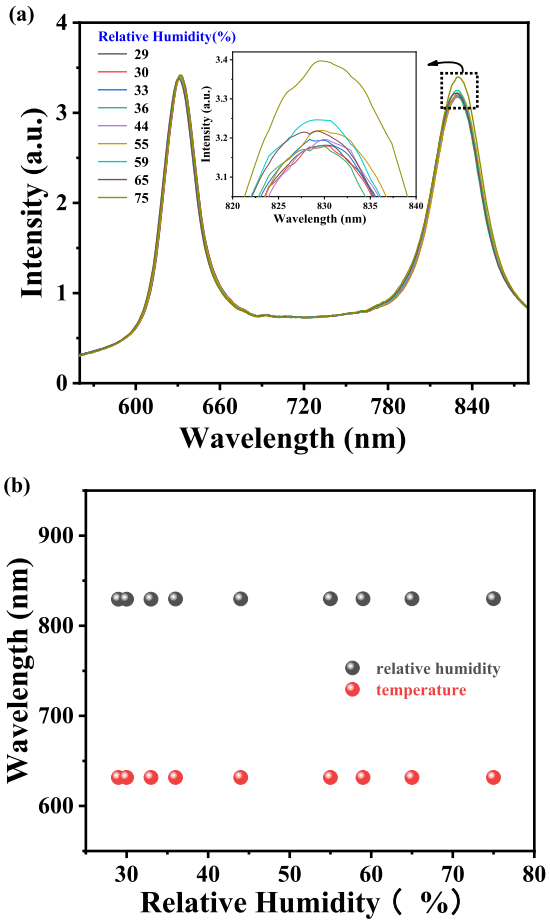

Fig. 7. (a) Reflection spectra of CLCs under increasing humidity; (b) Humidity dependences of CLCs reflection wavelength.

with probes in air chamber as the concentration repeatedly switched from 0 ppm to 6090 ppm. The maximum wavelength deviations at the two concentrations are 0.226 nm and 2.029 nm. Results in acetone of 6090 ppm appear an error fluctuation of 18%. This is because acetone leaks from air chamber when the probes are taken out during the continuous measurements, not because of quality of sensor. The decrease of acetone concentration, in effect, results in less wavelength shifts as described in Fig. 9(c). Our experimental results have verified that the sensor has good reversibility and repeatability for measuring acetone in both air and solution. A study on stability of sensor is finally conducted and shown in Fig. 9(d). Every few days we detected the acetone vapor in the same condition and analyzed the responses of gas probe within 32 days, the maximum deviation of probe sensitivity during the research is 7.1%, which proves that the sensor's performance in acetone monitoring is very stable. Table 1 shows the performance comparison of the sensors we propose with other sensors cited in the literature. Obviously, the proposed sensor has the advantage of gas and liquid dual use. In addition, the sensor has the advantages of small size and easy manufacturing. Therefore, the sensor has a broad application prospect in measurement.

4. Conclusions

In summary, by coating two fiber ends of a 2 × 2 multimode fiber coupler with CLCs of different reflection peaks, a gas-liquid two-phase fiber sensor with dual probes for detecting acetone and temperature was prepared. By monitoring the peak wavelength shifts at different acetone concentrations in air and solution, the sensitivities of the

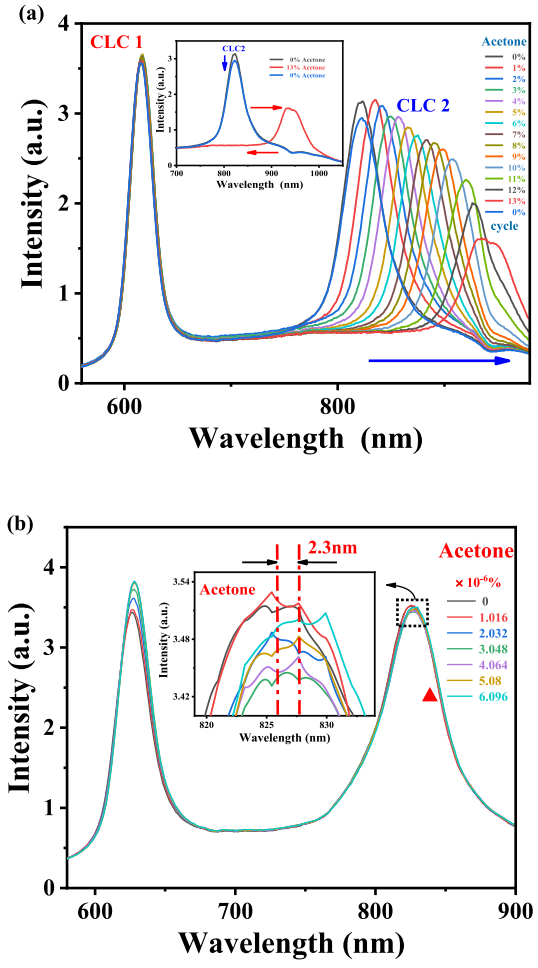

Fig. 8. (a) Detection range for acetone in solution; (b) Detection limit for acetone in solution.

Table 1
Several detection methods using liquid crystals.

Detection method	Qualitative/ quantitative assays	Application environment	Detection range	Ref.
LC cell	Qualitative	Gaseous	×	[19]
LC cell	Semi-quantitative	Gaseous	28.7 ppm~Hundreds ppm	[20]
Fiber optic sensing probes	Quantitative	Gaseous	630 ppm~378877 ppm	[21]
Fiber optic sensing probes	Quantitative	Liquid	0.5%~30%	[22]
Fiber optic sensing probes	Quantitative	Gas or liquid	308 ppm~50750 ppm 6.096 × 10^{-6}%~13%	our work

gas probe are 46.95 nm/mmol L^{-1} and 8.43 nm/%. The detection limits are 308 ppm, 6.096 × 10^{-6}% respectively. The sensitivity of the temperature probe is 2.44 nm/°C, and the measurable range is 24~40 °C, which is not affected by humidity. They both have good linearity, repeatability and stability. Acetone is an important raw material for chemical industry, it is toxic, soluble in water and volatile. Therefore, monitoring acetone leakage during storage or transportation is of great significance. Our proposed sensor can be used to monitor acetone in both gas and liquid phases at room temperature, it provides convenience for future industrial production.

Declaration of competing interest

The authors declare that they have no known competing financial interests or personal relationships that could have appeared to influence the work reported in this paper.

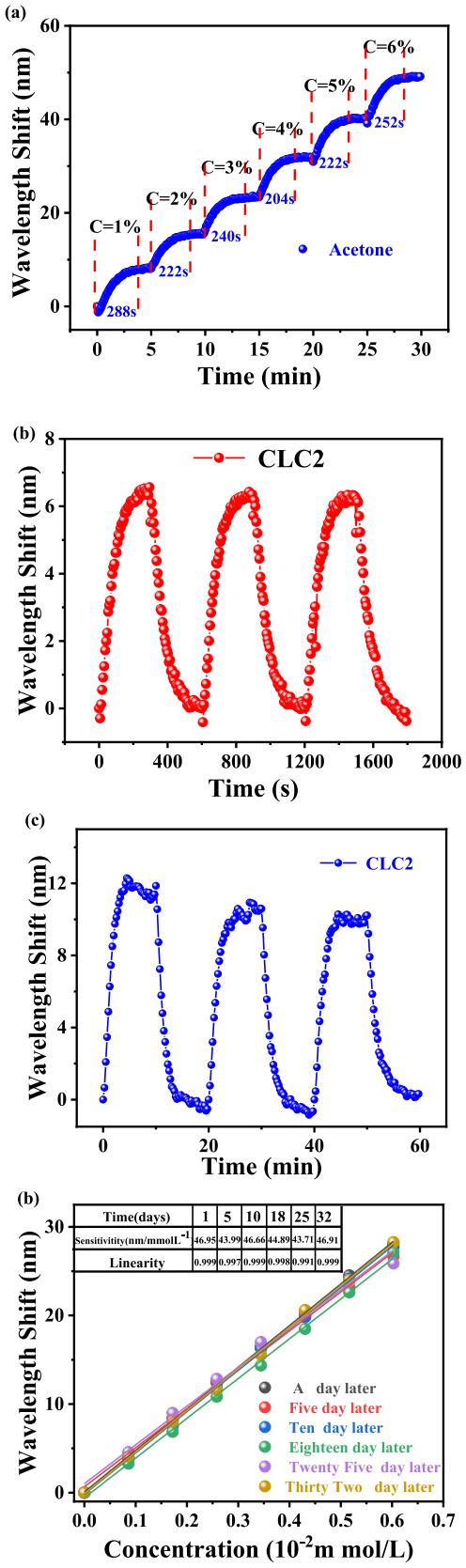

Fig. 9. (a) The response time of the sensor to different concentrations of acetone in aqueous solution; (b) The repeatability of the sensor when the acetone concentration is 0% or 1%; (c) When the concentration of acetone vapor is 0 ppm or 6090 ppm, the repeatability of the sensor; (d) Research on the stability of the sensor in 32 days.

Data availability

Data will be made available on request.

Acknowledgments

This work was financially supported by the National Science Foundation of China (Grant No. U1531102, 61975202, 61107059), the Fundamental Research Funds for the Central Universities, China.

References

[1] M.R. Loos, L.A.F. Coelho, S.H. Pezzin, S.C. Amico, The effect of acetone addition on the properties of epoxy, Polímeros 18 (2008) 76–80, http://dx.doi.org/10.1590/s0104-14282008000100015.

[2] Q.X. Yu, J.H. Zhu, Z.Y. Xu, X.T. Huang, Facile synthesis of alpha-Fe2O3@SnO2 core–shell heterostructure nanotubes for high performance gas sensors, Sensor Actuat. B-Chem. 213 (2015) 27–34, http://dx.doi.org/10.1016/j.snb.2015.01.130.

[3] S.F. Bamsaoud, S.B. Rane, R.N. Karekar, R.C. Aiyer, Nano particulate SnO2 based resistive films as a hydrogen and acetone vapour sensor, Sensors Actuators B 153 (2011) 382–391, http://dx.doi.org/10.1016/j.snb.2010.11.003.

[4] S. Salehi, E. Nikan, A.A. Khodadadi, Y. Mortazavi, Highly sensitive carbon nanotubes–SnO2 nanocomposite sensor for acetone detection in diabetes mellitus breath, Sensors Actuators B 205 (2014) 261–267, http://dx.doi.org/10.1016/j.snb.2014.08.082.

[5] S. Shao, H. Wu, S. Wang, Q. Hong, R. Koehn, T. Wu, W.-F. Rao, Highly crystalline and ordered nanoporous SnO2 thin films with enhanced acetone sensing property at room temperature, J. Mater. Chem. C 3 (2015) 10819–10829, http://dx.doi.org/10.1039/c5tc02188j.

[6] Q. Jia, H. Ji, Y. Zhang, Y. Chen, X. Sun, Z. Jin, Rapid and selective detection of acetone using hierarchical ZnO gas sensor for hazardous odor markers application, J.azard. Mater. 276 (2014) 262–270, http://dx.doi.org/10.1016/j.jhazmat.2014.05.044.

[7] S.T. Navale, Z.B. Yang, C. Liu, P.J. Cao, V.B. Patil, N.S. Ramgir, R.S. Mane, F.J. Stadler, Enhanced acetone sensing properties of titanium dioxide nanoparticles with a sub-ppm detection limit, Sensors Actuators B 255 (2018) 1701–1710, http://dx.doi.org/10.1016/j.snb.2017.08.186.

[8] T.T. Zhou, T. Zhang, Y. Zeng, R. Zhang, Z. Lou, J.N. Deng, L.L. Wang, Structure-driven efficient NiFe2O4 materials for ultra-fast response electronic sensing platform, Sensor. Actuat. B-Chem. 255 (2018) 1436–1444, http://dx.doi.org/10.1016/j.snb.2017.08.139.

[9] P. Jedlovszky, A. Idrissi, G. Jancso, Can existing models qualitatively describe the mixing behavior of acetone with water?, J. Chem. Phys. 130 (2009) http://dx.doi.org/10.1063/1.3086859.

[10] A.M. Diskin, P. Spanel, D. Smith, Increase of acetone and ammonia in urine headspace and breath during ovulation quantified using selected ion flow tube mass spectrometry, Physiol. Meas. 24 (2003) 191–199, http://dx.doi.org/10.1088/0967-3334/24/1/314.

[11] D. Smith, K.M.K. Ismail, A.M. Diskin, G. Chapman, J.L. Magnay, P. Spanel, S. O'Brien, Increase of acetone emitted by urine in relation to ovulation, Acta Obstet. Gyn. Scan. 85 (2006) 1008–1011, http://dx.doi.org/10.1080/00016340600590535.

[12] Y.J. Yoon, Y.J. Jung, B.S. Han, J.W. Kang, Performance of electron beam irradiation for treatment of groundwater contaminated with acetone, Water Sci. Technol. 59 (2009) 2475–2483, http://dx.doi.org/10.2166/wst.2009.234.

[13] R.S. Khadayate, V. Sali, P.P. Patil, Acetone vapor sensing properties of screen printed WO3 thick films, Talanta 72 (2007) 1077–1081, http://dx.doi.org/10.1016/j.talanta.2006.12.043.

[14] J.-S. Jang, S.-J. Choi, S.-J. Kim, M. Hakim, I.-D. Kim, Rational design of highly porous SnO2Nanotubes functionalized with biomimetic nanocatalysts for direct observation of simulated diabetes, Adv. Funct. Mater. 26 (2016) 4740–4748, http://dx.doi.org/10.1002/adfm.201600797.

[15] I. Ueta, Y. Saito, M. Hosoe, M. Okamoto, H. Ohkita, S. Shirai, H. Tamura, K. Jinno, Breath acetone analysis with miniaturized sample preparation device: In-needle preconcentration and subsequent determination by gas chromatography-mass spectroscopy, J. Chromatogr. B Analyt. Technol. Biomed. Life Sci. 877 (2009) 2551–2556, http://dx.doi.org/10.1016/j.jchromb.2009.06.039.

[16] A. Mirzaei, J.H. Kim, H.W. Kim, S.S. Kim, Resistive-based gas sensors for detection of benzene, toluene and xylene (BTX) gases: A review, J. Mater. Chem. C 6 (2018) 4342–4370, http://dx.doi.org/10.1039/c8tc00245b.

[17] V.K. Sharma, D. Mohan, P.D. Sahare, Fluorescence quenching of 3-methyl 7-hydroxyl Coumarin in presence of acetone, Spectrochim. Acta. A 66 (2007) 111–113, http://dx.doi.org/10.1016/j.saa.2006.02.032.

[18] C.K. Chang, C.W.M. Bastiaansen, D.J. Broer, H.L. Kuo, Discrimination of alcohol molecules using hydrogen-bridged cholesteric polymer networks, Macromolecules 45 (2012) 4550–4555, http://dx.doi.org/10.1021/ma3007152.

[19] H. Xu, F. Baldini, K.-L. Yang, J. Homola, R.A. Lieberman, Using liquid crystals as optical gas sensors to detect thiol vapors, Opt. Sensors 2009 (2009) http://dx.doi.org/10.1117/12.819892.

[20] C.-K. Chang, H.-L. Kuo, K.-T. Tang, S.-W. Chiu, Optical detection of organic vapors using cholesteric liquid crystals, Appl. Phys. Lett. 99 (2011) http://dx.doi.org/10.1063/1.3627162.

[21] Y.H. Yang, D. Zhou, X.J. Liu, Y.J. Liu, S.Q. Liu, P.X. Miao, Y.C. Shi, W.M. Sun, Optical fiber sensor based on a cholesteric liquid crystal film for mixed VOC sensing, Opt. Express 28 (2020) 31872–31881, http://dx.doi.org/10.1364/Oe.405627.

[22] Y.M. Su, Z.Q. Lan, J.M. Wang, L. Zeng, D. Zhou, Z.H. Peng, W.M. Sun, Y.J. Liu, Optical fiber sensor for determination of methanol ratio in methanol-doped ethanol based on two cholesteric liquid crystal droplets embedded in Chitosan, J. Lightwave Technol. 39 (2021) 5170–5176, http://dx.doi.org/10.1109/Jlt.2021.3078744.

[23] C. Esteves, E. Ramou, A.R.P. Porteira, A.J.M. Barbosa, A.C.A. Roque, Seeing the unseen: The role of liquid crystals in gas-sensing technologies, Adv. Opt. Mater. 8 (2020) http://dx.doi.org/10.1002/adom.201902117.

[24] R. Kanavvade, A. Kumar, D. Pawar, K. Vairagi, D. Late, S. Sarkar, R.K. Sinha, S. Mondal, Negative axicon tip-based fiber optic interferometer cavity sensor for volatile gas sensing, Opt. Express 27 (2019) 7277–7290, http://dx.doi.org/10.1364/Oe.27.007277.

[25] M. Humar, Liquid-crystal-droplet optical microcavities, Liq. Cryst. 43 (2016) 1937–1950, http://dx.doi.org/10.1080/02678292.2016.1221151.

[26] A. Shrivastava, V. Gupta, Methods for the determination of limit of detection and limit of quantitation of the analytical methods, Chronicles Young Sci. 2 (2011) http://dx.doi.org/10.4103/2229-5186.79345.

[27] H. Zhang, J.Y. Shang, X.J. Liu, W.M. Sun, F.R. Wang, Y.J. Liu, High-sensitivity fiber liquid crystals temperature sensor with tiny size and simple tapered structure, Chin. Opt. Lett. 18 (2020) http://dx.doi.org/10.3788/Col202018.101202.

[28] J.Y. Hu, Y.Z. Chen, Z.Y. Ma, L. Zeng, D. Zhou, Z.H. Peng, W.M. Sun, Y.J. Liu, Temperature-compensated optical fiber sensor for volatile organic compound gas detection based on cholesteric liquid crystal, Opt. Lett. 46 (2021) 3324–3327, http://dx.doi.org/10.1364/Ol.427606.